Development of Solder Joint Inspection Method using Air Stimulation Speckle Vibration Detection Method and Fluorescence Detection Method

Takashi Hiroi, Kazushi Yoshimura, Takanori Ninomiya, Toshimitsu Hamada*1), Yasuo Nakagawa,
Production Engineering Research Laboratory, Hitachi Ltd.
292 Yoshida-cho, Totsuka-ku, Yokohama 244, Japan,
Shigeki Mio, Kouichi Karasaki, and Hideaki Sasaki,
General Purpose Computer Division, Hitachi Ltd.
1 Horiyamashita, Hadano, Kanagawa 259-13, Japan.

ABSTRACT

A fast and highly reliable method of inspecting minute solder joints of high-density mounted devices has been developed. It uses two techniques to detect all types of defects, such as unsoldered leads, solder bridges, and mis-aligned leads. One applies external force to solder joints with an air jet, which vibrates or shifts unsoldered leads. The vibration and shift is detected as a change in the speckle pattern produced by laser illumination of the solder joints. The other uses fluorescence from PC (Printed circuit) boards generated by short wavelength laser illumination. A silhouette image of the solder joint is detected and processed to extracts defects. The experimental results show that this new inspection method detects all types of defects accurately with a very low false alarm rate.

1. INTRODUCTION

Great progress has recently been made in high density packaging and fine soldering technology. Despite efforts to achieve perfect soldering, the occurrence of defects is still unavoidable. Consequently, post-soldering inspection is indispensable. Many methods have been reported; Thermal radiation detection [1] heats solder joints with a laser and detects transitional thermal radiation. Shape from specular [2-6] detects surface orientation of soldered surfaces using direct reflection of illuminated light. X-ray image detection [7] detects transmitted X-rays. Mechanical impedance detection [8] detects the impedance spectrum of vibration caused by a contact vibrator. The photothermoelastic [9] detects thermal changes caused by a laser pulse. The light sectioning method detects the profile of a solid solder joint by slit light projection [10] or co-diffraction of a spot light and a linear image sensor [11]. In applying these methods for high density packaging, the following problems should be considered. The thermal radiation detection method is very sensitive to surface orientation and its reflectivity. Optical methods, which try to detect the solid shape, such as the shape-from-specular methods and light-sectioning method, require a wide detection angle and stable reflectance, but these not can be expected to detect the shape accurately when there is a narrow gap between tall devices and a big intensity change caused by a minor change of surface orientation. Besides the information of both solder joints, an X-ray image contains and dozens of internal layers, and it is difficult to distinguish solder joints. The mechanical impedance method may damage solder joints by physical contact probing. The photothermoelastic method is also very sensitive to lead shape and surface reflectivity. Thus, it is very difficult to use these conventional methods for a reliable inspection of solder joints on a high density PC board. We have developed a new solder joint inspection method.

2. INSPECTION OBJECTS AND DEFECTS TO BE DETECTED

Figure 1 shows part of a mounted PC board and the solder joints. The devices are 17 mm high and the minimum gap between them is about 4 mm. The inspection objects are the solder joints of QFP (Quad Flat Package) gull-wing leads on the board, which have 0.5-mm lead pitch and 0.2-mm lead width as shown in Fig. 1(b). There are three major defects: unsoldered leads, solder bridges, and mis-aligned leads. These defects are categorized into two different groups. The first one is unsoldered leads, which are very difficult to identify from their appearances, so a human inspector must check them with a microscope, sometimes by sticking them with a pair of tweezers. The second group is solder bridges and mis-aligned leads which can be seen in two-dimensional images.

As these two groups are radically different from each other.

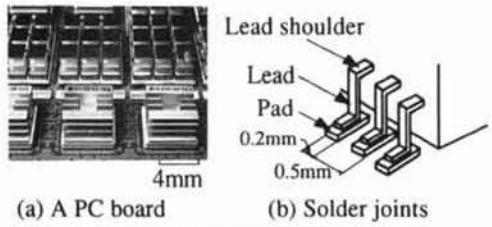

(a) A PC board (b) Solder joints

Fig. 1 Inspection objects

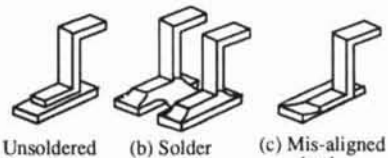

(a) Unsoldered lead (b) Solder bridge (c) Mis-aligned lead

Fig. 2 Defects to be detected

Therefore, two individual methods were developed for them and combined to detect all defects. One is an air stimulation laser speckle vibration detection method [12] for detecting unsoldered leads. The other is a fluorescence detection method, which was originally developed for PC board pattern inspection [13], that we modified for detecting solder bridges and misaligned leads.

3. AIR STIMULATION LASER SPECKLE VIBRATION DETECTION METHOD

DETECTION PRINCIPLE

The principle of this method is shown in Fig. 3. Solder joints are stimulated by an air jet from an oblique direction. A well soldered lead does not move at all, because it is firmly fixed to the PC board by soldering. On the other hand, an unsoldered lead, which is not in contact with a pad on a board is vibrated by the air stimulation. This vibration is detected as a change in a laser speckle when the lead is illuminated by a laser. Speckle is a random pattern caused by interference of reflected laser light and it is detected on a defocal plane. It is very sensitive to changes in location or orientation of the lead surface. Figure 3 also shows examples of speckle patterns of solder joints stimulated by air jet. The speckle pattern of a well-soldered lead has high contrast spots and is not affected by the air stimulation. But the speckle pattern of an unsoldered lead changes as the lead vibrates and is detected as a blurred pattern due to time integration effect of an image sensor. Some unsoldered leads which are in contact with pads do not vibrate but shift, and these speckle patterns also shift according to these movements. Therefore, shift of speckle patterns as well as blur must be extracted from the speckle pattern image.

BASIC ANALYSIS

We analyzed the speckle pattern movement theoretically and experimentally. The amount of orientation change of lead's toe due to it's shift and vibration exceeded 1 mrad and vibration frequency is 10-20 kHz, under air stimulation at 200 kPa from a 20-mm height and 45 degree oblique direction. Speckle movement caused by the lead shift was analyzed. Assuming that the intensity distribution of speckle patterns before and after movement are $I_1(x_1,y_1)$ and $I_2(x_2, y_2)$ respectively and that relative correlation of I_1 and I_2 is maximum at (x_2,y_2) equal (x_1+A_x,y_1+A_y), then A_x and A_y which mean speckle movement measure are given by

$$A_x=-a_x\times m-\frac{2\theta_y\times\delta}{m} \quad \cdots (1)$$

$$A_y=-a_y\times m-\frac{2\theta_x\times\delta}{m}$$

where a_x and a_y are movements of the object, θ_x and θ_y are orientation changes, and δ is the defocal distance, i.e., the distance between the image detection plane and the focal plane as shown in Fig. 4 [14].

The speckle movement was measured experimentally. Figure 5 contains the theoretical calculations (lines) and experimental values (points). Speckle movements are proportional to the change in the object's orientation θ_x and θ_y and defocal distance δ, and the experimental results agree well with the theoretical calculations.

CONFIGURATION OF THE DETECTION HEAD

The configuration of the detection head is shown in Figure 6 and its specifications are given in Table 1. All solder joints located on one side of a QFP, in a row, are detected at the same time. Solder joints are illuminated over a width of 20 mm by the Ar laser and are stimulated by an air jet pulse from two sets of 20 mm wide slit nozzles, which are arranged obliquely toward leads. The intensity of the speckle patterns is detected by a linear image sensor.

Detected speckle intensities vary according to the orientation and reflectivity of leads. Figure 7 shows a histogram

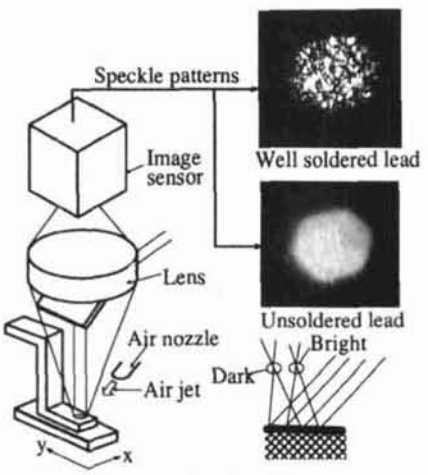

Fig .3 Detection principle

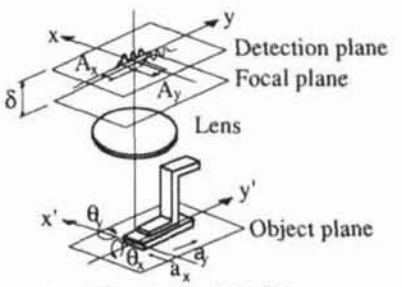

Fig. 4 Coodinate definition

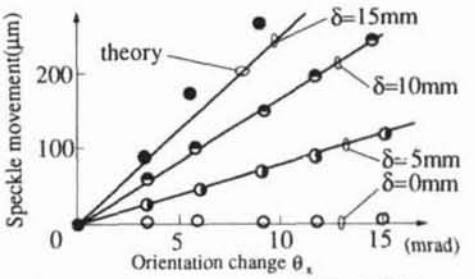

Fig. 5 Speckle movement with lead shift

of detected intensities. The horizontal axis shows the intensity, relative to sensor saturation level. The variation was from 10 % of saturation level to over saturation and to detect all leads adequately with same condition, intensity control is required. For this purpose, a liquid crystal filter was inserted just before the image sensor, and intensity of each leads is regulated by changing the transmittance distribution of the filter.

The configuration is shown in Figure 6 and the specifications of the liquid crystal filter are given Table 2. This filter has a series of electrode stripes which are controlled to obtain desired transmittance distribution. The control sequence of the filter is as follows.

1) The same low voltage is supplied to all electrodes to get a constant low transmittance ratio ϕ_0.
2) The intensity f(x) is detected by the image sensor, where x is the pixel index of the sensor.
3) The distribution of transmittance ratio $\phi(\xi)$ is calculated by

$$\phi(\xi)=\phi_0\frac{I_0}{\max(f(x)|x\in\xi)} \quad \cdots(2)$$

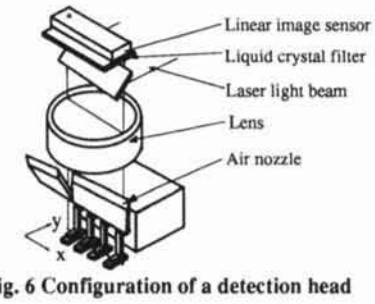

Fig. 6 Configuration of a detection head

Table 1 Specifications of detection head

air nozzle	24 mm wide slit 120 ms injection time 200 kPa supply pressure
laser source	Ar laser: λ=488 nm,power 0.5 W
illumination stripe	area: 24 mm x 0.3 mm
lens	focal length f=150 mm, F=2.8 magnification m=1.2
defocus	δ=10 mm, with cylindrical lens of f=40 mm
intensity control	liquid crystal filter
image sensor	clock 4 MHz, integration time:1 ms pixel size:8 μm, 3648 pixels

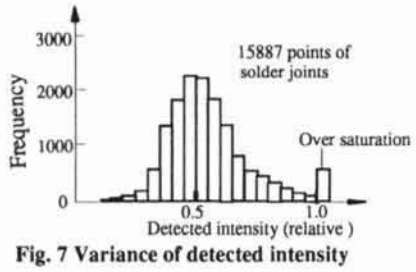

Fig. 7 Variance of detected intensity

where I_0 is the desired intensity and x is pixel index of the image sensor which corresponds to a filter electrode ξ.

Figure 9 shows the intensity histogram regulated by this filter. The range of intensity variation was regulated satisfactorily between 0.27 and 0.68.

ALGORITHM

Figure 10 shows examples of detected speckle patterns. This figure shows the transitional intensity of the speckle patterns of 5 solder joints, which are shown in the microscope photograph above. The horizontal axis of the figure is the pixel index of the image sensor and the vertical axis is time. The speckle waveform of the unsoldered lead is blurred just after the air jet is applied. On the other hand, the speckle waveform of the well soldered lead is constant.

The leads are judged by comparing the waveforms before and after. We introduce a vibration evaluation function G(x) which indicates the transition of the high frequency component of the two waveforms and shift evaluation function H(x) which indicates the difference between the two waveforms.

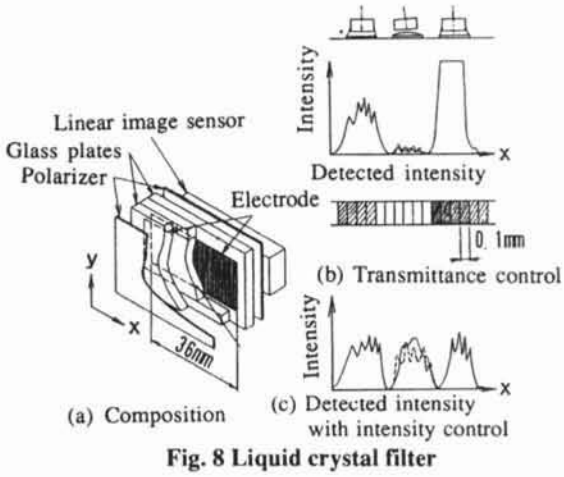

Fig. 8 Liquid crystal filter

Table 2 Specifications of liquid crystal filter

electrode	0.1 mm pitch x 5 mm, 360 pixels
bright/dark ratio	120 (wavelength λ= 488nm, vertical incident)
transmittance	maximum 68 % (same as above)
sel gap	9 μm, ΔND=0.96

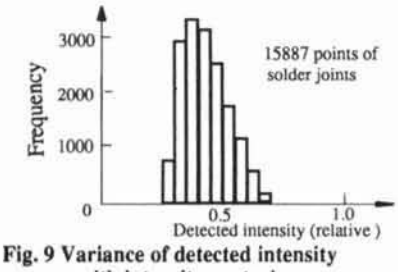

Fig. 9 Variance of detected intensity with intensity control

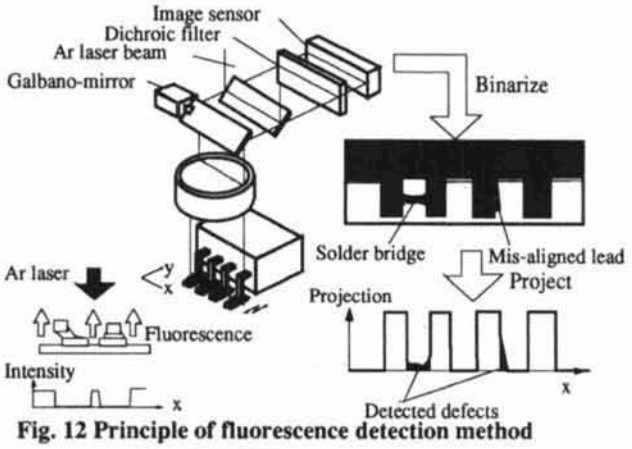

Fig. 12 Principle of fluorescence detection method

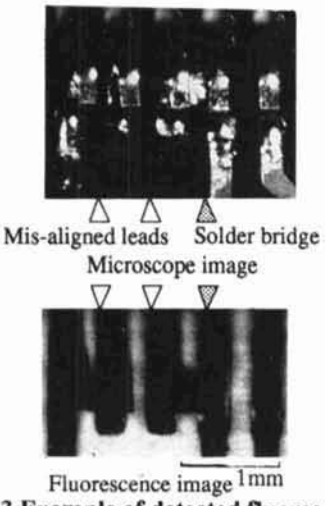

Fig. 13 Example of detected fluorescence image

5. CONFIGURATION OF A INSPECTION SYSTEM

Figure 14 illustrates the configuration of our inspection system, which combines both detection methods. Ar laser with wavelength 488nm illuminates to the objects through a galvano-mirror and reflected light is detected by the sensor-S for speckle detection and fluorescence light is detected through a dichroic filter by the sensor-F.

The inspection sequence is as follows. First, the galvano-mirror is scanned, and a two-dimensional fluorescence image is detected, and from this image solder bridges and mis-aligned leads are judged. Then, the galvanometer is positioned to illuminate the center of solder joints. Leads are stimulated by an air jet pulse, and speckle waveforms before and after air jet stimulation are detected. From these waveforms, unsoldered leads are judged. These fluorescence image and speckle waveforms are processed by hardware which is controlled by microprocessors. And a whole system is controlled by a mini-computer. Figure 15 shows a photograph of the inspection system, which can inspect all types of solder joints at a rate of 70ms per a lead.

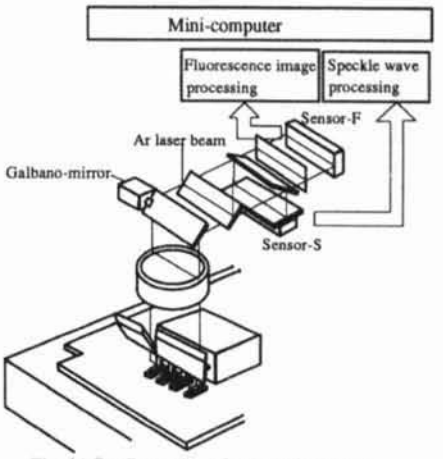

Fig. 14 Configuration of a detection head

Fig. 15 Inspection system

6. EXPERIMENTAL RESULTS

Figure 16 shows a tested PC board, whose size is 420 mm x 280 mm. Figure 17 shows judgment results for the 10,034 solder joints by the speckle detection method, where the horizontal axis of the figure is the vibration evaluator G_1 and the vertical axis is the shift evaluator H_1. This figure shows the population for each evaluator value. The judgment threshold S_{th} was set to 0.25. All of the 44 unsoldered leads were detected, and 6 well soldered leads were wrongly detected, so its false detection ratio is 0.06%, and 9,193 out of 9,990 good leads are located on $H_1=G_1=0$. The reason for the false detection of well-soldered lead is that a lead shoulder of the lead comes into the detection area and its vibration is mistaken for that of an unsoldered lead.

Figure 18 shows the accuracy of detected lead gaps by the fluorescence detection method. The horizontal axis is the actual lead gap and the vertical axis is the detected gap value. If the lead height is less than 500 μm, gap detection accuracy is ±20 μm, which is sufficient to measure a lead gap and detect a mis-aligned lead. Figure 19 shows the detection performance for solder bridges. Metallic wires which had the same surface conditions as those of solder bridges was used for the evaluation. The horizontal axis is wire height and the vertical axis is detected intensity ratio. Wires are detectable when the ratio R is less than 0.5. If the wire height is less than 500-μm, 25-μm wire can be detected. Because an actual solder bridge is generally located on a surface of PC board and its width is larger than 100 μm. Experimental results guarantee almost

(1) Vibration evaluation function G(x)

We extract the high frequency component of the speckle waveforms, whose pitch is about 4 pixels, by using the 2nd order differential, which is given by

$$f''(x)=f(x-2)+f(x-1)-2f(x)-2f(x+1)+f(x+2)+f(x+3). \quad \cdots (3)$$

Using this differential, vibration evaluation function G(x) is defined by

$$G(x)=\frac{\sum_{\xi=x-\Delta}^{x+\Delta}|f''_0(\xi)|-\sum_{\xi=x-\Delta}^{x+\Delta}|f''_1(\xi)|}{\sum_{\xi=x-\Delta}^{x+\Delta}|f''_0(\xi)|} \cdots \quad \cdots (4)$$

where $f_0(x)$ and $f_1(x)$ are speckle waveforms before and after the air jet.

G(x) increases when speckle waveform becomes blurred by the air jet.

(2) Shift evaluation function H(x)

The difference between two waveforms is obtained using a simple shift measure, which is given by

$$H(x)=\frac{\sum_{\xi=x-\Delta}^{x+\Delta}|f''_0(\xi)|+f''_0(\xi+1)-|f''_1(\xi)|-f''_1(\xi+1)|}{\sum_{\xi=x-\Delta}^{x+\Delta}|f''_0(\xi)+f''_0(\xi+1)|}, \cdots \cdots (5)$$

H(x) increases when two waveforms are different at x.

(3) Defect judgment

The unsoldered leads are judged based on the number of blurred or shifted pixels (see Fig. 11). The number of pixels which have larger G(x) or H(x) than each threshold H_{th} and G_{th}, is counted and the ratio of the number against that of all pixels is calculated for each solder joint. We call the ratio of G(x) *the vibration evaluator* G_1 and the ratio of H(x) *the shift evaluator* G_1. The defect evaluator S is defined by

$$S=\max(G_{1R},G_{1L})+\max(H_{1R},H_{1L}) \cdots \quad \cdots (6)$$

where suffix R means the evaluator by the right nozzle and L means the evaluator by left one.

Solder joints with S larger than judgment threshold level S_{th} are judged to be unsoldered leads.

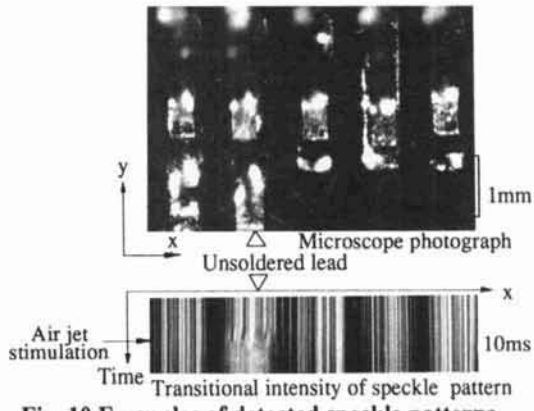

Fig. 10 Examples of detected speckle patterns

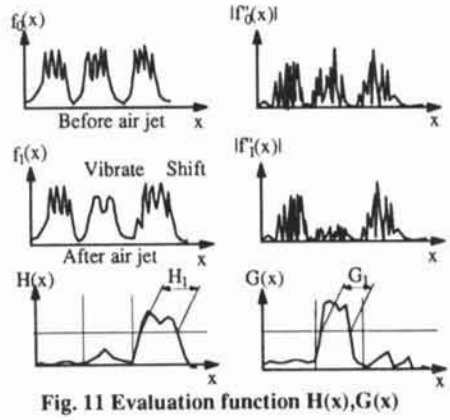

Fig. 11 Evaluation function H(x),G(x)

4. FLUORESCENCE DETECTION METHOD

The principle of the developed fluorescence detection method is shown in Fig. 12. Fluorescence from insulator of a PC board is excited by short-wavelength laser illumination and is detected through a dichroic filter. The fluorescence is only generated from organic material and a silhouette image of the solder joints can be obtained. Figure 13 shows a fluorescence image and an ordinary microscope image. Although solder joints have a specular surface in the ordinary image, a stable high contrast image can be obtained by fluorescence detection. The detected fluorescence image is thresholded and projected in the y-axis direction as shown in Fig. 12. The projection waveform is compared with design rules, that lead and pad must be located apart from a neighboring pad with at least minimum spacing criteria. And solder bridge is extracted as no gap between solder joints and mis-aligned lead is extracted as a smaller than expected gap.

perfect detection of the actual solder bridges.

After this evaluation, we applied the inspection system to a practical production line and obtained good results.

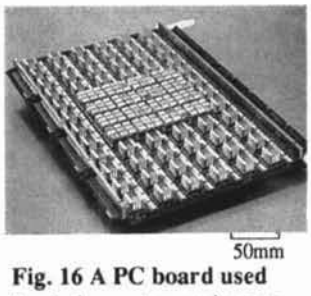

Fig. 16 A PC board used for judgment experiments

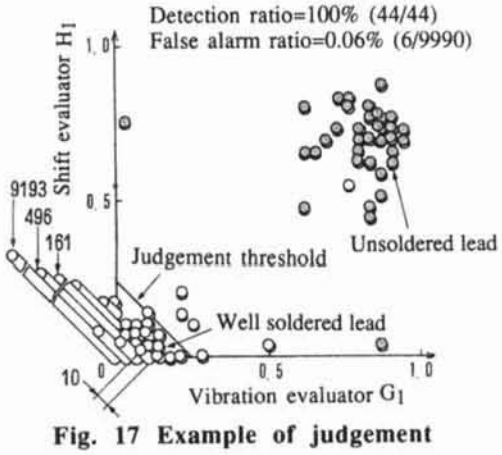

Fig. 17 Example of judgement

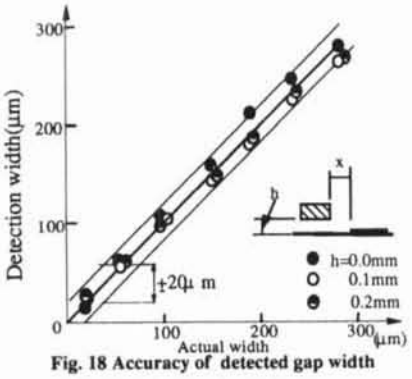

Fig. 18 Accuracy of detected gap width

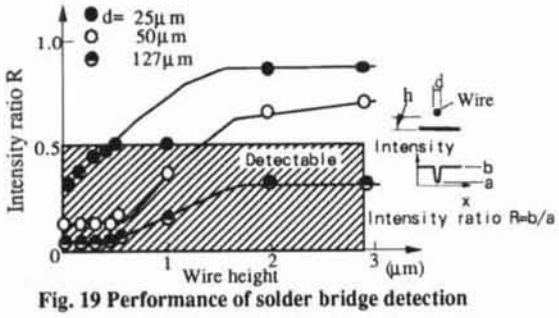

Fig. 19 Performance of solder bridge detection

7. CONCLUSION

We have developed two methods for detecting defects of minute solder joints on a high density PC board. One method appling an external force to solder joints to induce vibration or shift in an unsoldered lead and detects the vibration and shift as a change in the speckle pattern produced by laser illumination. The other detects fluorescence caused by short-wavelength laser illumination, obtains a silhouette image of the solder joints, thresholds the image, then takes a projection to determine defects. The result shows this new inspection method can detect all types of defects accurately with a very low false alarm rate. The combination of these two methods is a useful solution to the problem of inspecting minute solder joints on a high density PC board.

ACKNOWLEDGEMENT

The authors wish to thank to Tassei Sagawa*2) and Yasuhiko Satoh*2) for their kind suggestions and support in this study and to Yasuo Takenaka*3) for joint effort in developing the inspection system.

REFERENCES

[1] Riccardo Vanzetti, Alan Traub:"Automated Laser Inspection of Solder Joints", ISTFA, pp. 85-96, '81.

[2] D.W.Capson, Sai-Kit Eng:"A Tired Color Illumination Approach for Visual Inspection of Solder Joints", Proceeding of Vision '86, pp. 3.57-3.72, '86.

[3] Paul Besl, Edward Delp, Ramesh Jain:"Automatic Visual Inspection of Solder Joints", IEEE J. Robotics Automation, pp. 467-473, '85.

[4] Shigeki Kobayashi:"Automatic Solder Joint Inspection Utilizing Color Illumination", JSPE, Vol. 56, No. 8, pp.1375-1380, '90, (in Japanese).

[5] C.Sanderson, Lee E. Weiss and Shree K. Nayar:"Structured Highlight Inspection of Specular Surface",IEEE Trans. PAMI, PAMI-10, No. 1, pp. 44-55, '88.

[6] S.K.Nayar and A.C.Sanderson:"Detection Surface Orientaions of Specular Surfaces by Intensity Encoded Illumination", Proc. of SPIE vol. 850, pp. 122-127, '87.

[7] Mike Juha:"why X-Ray Inspection for Solder Quality Must be Automated",Technical Paper Society of Manufacturing Engineers", No. EE-86-305, pp. 1-17, '86.

[8] Dale Ensminger:"Inspection of Solder Joints by Acoustic Impedance", U.S.Patent, 4,287,766, pp.1-5, '81

[9] Kazuhiro Hane and Syuzo Hattori:"Photothermoelastic Inspection of Soldered Connections",Appl. Opt., Vol. 27, No. 19, pp. 3965-3967, '88.

[10]Yasuo Nakagawa:"Automatic Visual Inspection of Printed Circuit Boards",Proceeding of SPIE, Vol. 336, Robot Vision, pp. 121-127, '82.

[11]Yasuo Nakagawa, Yoshitada Oshida, Takanori Ninomiya, and Hideaki Sasaki:"Shapre Detection of Solder Joints by Spotlight Scanning Light-Section Method", Vol. 22, No. 9, SICE, '86.

[12]Takashi Hiroi, Kazushi Yoshimura, Toshimitsu Hamada, Takanori Ninomiya, Yasuo Nakagawa, Shigeki Mio, Hideaki Sasaki:"Development of Solder Joint Inspection Method Using Air Stimulation/Speckle Vibration Detection Method", T.IEE, Vol. 112-C, No. 2, pp. 125-134, '92, (in Japanese).

[13]Yasuhiko Hara:"A System for PCB Automated Inspection Using Fluorescence Light",Pattern Recognition, Vol. 10, No. 1, pp. 69-78, '88.

[14]Ichiro Yamaguchi:"Deformation Measurement for Diffusely Reflecting Objects by Lasers", Japanese Journal of Applied Physics, Vol. 48, No. 3, pp. 17-31, '79, (in Japanese).

*1) Current address; Headquarters Sales Office, Hitachi Ltd. 4-6 Kanda-Surugadai, Chiyoda-ku, Tokyo 101, Japan

*2) General Purpose Computer Division, Hitachi Ltd.

*3) Hitachi Electric Engineering Ltd.